A Novel Engine Architecture for Low NOx Emissions

Blondeel, Tim; Yin, Feijia; Rao, Arvind Gangoli

DOI
10.1115/GT2022-81738

Publication date
2022

Document Version
Final published version

Published in
Aircraft Engine; Ceramics and Ceramic Composites

Proceedings of ASME Turbo Expo 2022
Turbomachinery Technical Conference and Exposition
GT2022
June 13-17, 2022, Rotterdam, The Netherlands

GT2022-81738

A NOVEL ENGINE ARCHITECTURE FOR LOW NO_x EMISSIONS

Tim Blondeel, Feijia Yin, Arvind Gangoli Rao
Faculty of Aerospace Engineering, Delft University of Technology, Delft, the Netherlands

ABSTRACT

The fuel efficiency of turbofan engines has improved significantly, hence reducing aviation's CO_2 emissions. However, the increased operating pressure and temperature for fuel efficiency cause adverse effects on NO_x emissions. Therefore, a novel engine concept, which can reduce NO_x emissions without affecting the cycle efficiency, is of high interest to the aviation community. This paper investigates the potential of an intercooler and inter-turbine burner (ITB) for the future low NO_x aircraft propulsion system.

The study evaluates performance and NO_x emissions of four engine architectures: a very high bypass ratio (VHBR) turbofan engine (baseline), a VHBR engine with intercooler, a VHBR engine with ITB, and a VHBR engine with both intercooler and ITB. The cycles are optimized for minimum cruise Thrust Specific Fuel Consumption (TSFC), considering the same design space, thrust requirements, and operational constraints. The ITB is only used during take-off to minimize cruise fuel consumption. The analysis shows that using an ITB solely, with the energy split of 75% (the first burner) / 25% (ITB), reduces the cruise NO_x emission by 26%, and the cruise TSFC slightly by 0.5%. The intercooler alone reduces the NO_x emissions by 16% and the cruise TSFC by 0.8%. The combination of intercooler and ITB reduces the NO_x emissions further by 38%. The analysis confirms that introducing an intercooler and ITB can potentially resolve the contradicting effects of fuel efficiency and NO_x emissions for the future advanced turbofan engine.

Keywords: Novel turbofan architecture, Intercooler, Inter-stage turbine burner, low NO_x emissions

NOMENCLATURE

BPR	Bypass ratio	
$EINO_x$	NO_x emission index	g/kg(fuel)/g/kN
FAR	Fuel to Air Ratio	
HPC	High Pressure Compressor	
HPT	High Pressure Turbine	
ITB	Inter-Turbine Burner	
LHV	Lower Heating Value	J/kg
LPC	Low Pressure Compressor	
LPT	Low Pressure Turbine	
$\dot{m}$	mass flow rate	kg/s
N1	Relative low-pressure spool speed	%
N2	Relative high-pressure spool speed	%
OPR	Overall Pressure Ratio	
ST	Specific thrust	kN/kg
TSFC	Thrust Specific Fuel Consumption	g/kN/s
VHBR	Very High Bypass Ratio	

1. INTRODUCTION

Aviation has become the backbone of our modern society in connecting the different parts of the world. The demand for air traffic increases annually by 4.4% [1]. Though growth has slowed down due to the COVID-19 crisis, we expect aviation, a fundamental part of long-range mobility, will eventually recover. As aviation continues growing, concerns on the environmental impact of aviation's emissions, e.g., CO_2 and NO_x, arise. CO_2 is a greenhouse gas. NO_x emissions in the landing take-off (LTO) cycle affect air quality near airports, whereas NO_x emissions at cruise level lead to global warming effects (via ozone formation and methane depletion process) [2]. To mitigate aviation's environmental impact, the European advisory body, ACARE, has set up stringent goals to reduce aviation's CO_2 emissions by 75% and NO_x emissions by 90% by 2050 compared to the baseline scenario of the year 2000 [3].

Over the past decades, technological development has reduced aviation's fuel burn (hence CO_2 emissions) per passenger kilometer by more than 70%. About 50% fuel reduction is achieved by the improvements of engine cycle efficiency [4], via various means, for instance, increasing engine overall pressure ratio (OPR), turbine inlet temperature, bypass ratio (BPR), etc. In modern aero engines, the BPR has reached 11, and the OPR has increased to 50, which leads to the further increase of the maximum operating temperature. Furthermore, the statistical analysis in Fig. 1 shows that increasing OPR causes an increase of engine NO_x emissions [5, 6] unless low NO_x combustion

techniques are applied, represented by the various regression curves. The sensitivity of NO_x emissions to engine OPR mainly relates to the increased combustor inlet pressure and temperature [7]. Therefore, novel engine configurations, which can reduce the dependency of NO_x emissions on the engine pressure ratio (thus fuel efficiency), would be of high interest to future aviation.

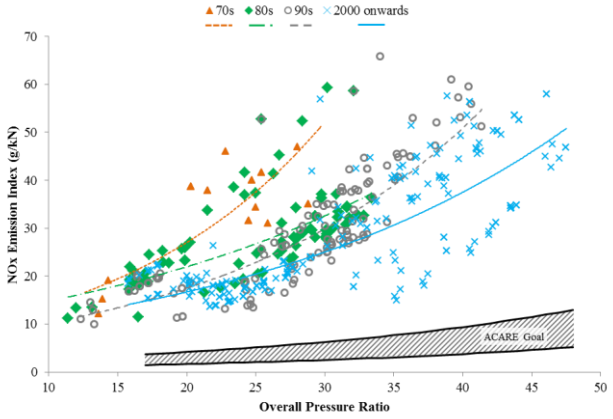

Figure 1: Variation of NO_x emission for given thrust versus engine overall pressure ratio [6].

The application of intercooler [8, 9] and inter-stage turbine burner (ITB) [4, 9] in aero engines have been studied previously for different interests. The feature of intercooler and ITB turbofan engines are briefly reviewed here.

- ***Intercooled turbofan engine***

The intercooler is a heat exchanger located between the low-pressure compressor (LPC) and the high-pressure compressor (HPC), as depicted in Fig. 2, to reduce the HPC inlet temperature.

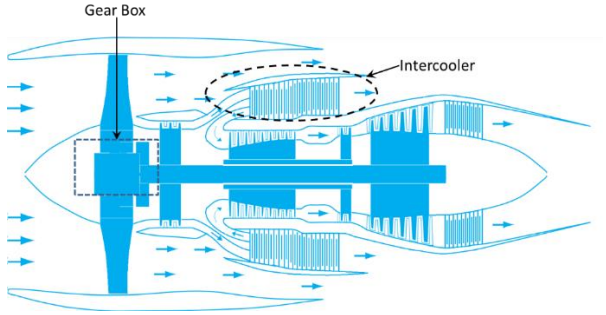

Figure 2: Schematic of a geared turbofan engine with intercooler.

Depending on the optimization strategy, the reduced HPC inlet temperature can have different effects. One possibility is to increase the engine OPR further without violating the temperature limits at the HPC exit, hence increasing fuel efficiency. However, this is typically limited by the blade height in the last compressor stage. Alternatively, one could maintain the OPR, thus reducing HPC exit temperature. Consequently, the amount of turbine cooling and the associated efficiency penalty decrease. Furthermore, the lower HPC exit temperature can reduce the thermal NO_x emissions.

Next to the advantages, challenges associated with the intercooler in aero engines require attention. For instance, pressure losses through the intercooler may deteriorate the cycle efficiency. This could be controlled by a proper heat exchanger design combined with the optimal pressure split between LPC and HPC. The intercooler leads to weight addition. The previous research [10] shows that the intercooler weight can be balanced with the weight reduction of the compressor and turbine.

- ***ITB turbofan engine***

The ITB is an additional combustion chamber between the high pressure turbine (HPT) and the low pressure turbine (LPT), allowing more freedom in engine cycle optimization. Figure 3 shows a schematic comparison of the ITB turbofan engine with the baseline engine. The envisaged design of ITB differs from the conventional combustion chamber for a more compact configuration and flow characteristics.

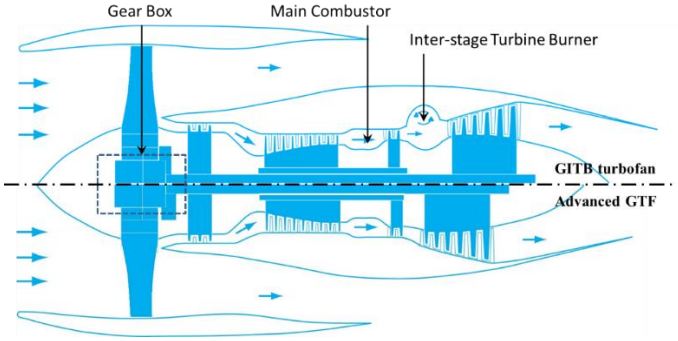

Figure 3: A comparison of a geared turbofan with ITB (GITB, upper half) to its baseline geared turbofan engine (GTF, lower half) [10].

The effects of ITB on engine performance were studied in the previous research [4, 11-13]. Similar to the intercooler, the additional power from ITB can have different effects. For instance, the specific thrust of the engine increases because of using ITB. Moreover, the NO_x emission can be reduced when the specific thrust is fixed for multiple reasons. First, ITB reduces the HPT inlet temperature, hence the thermal NO_x. Second, a part of the NO_x from the first combustor is dissociated in the ITB through the process of re-burning, reducing the overall NO_x emissions further [4, 14]. The previous research [15, 16] shows that the ITB can also facilitate low NO_x combustion techniques, such as flameless combustion [17], which would otherwise be impossible for aero-engines because of its need for elevated temperature large circulation zone. The lower HPT inlet temperature reduces the amount of turbine cooling [10].

While the previous research studies the effects of intercooler and ITB individually, an engine architecture with both has not been studied. This research proposes a novel engine architecture, i.e., an intercooler ITB turbofan engine, focusing on the combined effects of an intercooler and ITB on resolving the CO_2 and NO_x coupling issue. The paper starts with the modeling approach described in section 2, followed by the main research findings described in section 3, and is concluded by section 4.

2. ENGINE PERFORMANCE AND EMISSIONS MODELING

The engine model comprises performance calculation, optimization, and NO_x emission prediction. All the engines in this study are defined assuming the same technology level, i.e., turbomachinery efficiencies, component losses, maximum allowable pressure, and temperature.

2.1 The engine performance model

The baseline engine in this research is a future geared driven very high bypass ratio (VHBR) turbofan engine for a long-range mission. The engine layout is depicted in Fig. 4 with the station number. The engine performance requirement is derived based on the state-of-the-art GEnx-1B for B787 aircraft, as shown in Table 1. All the engines in this study are expected to meet these requirements.

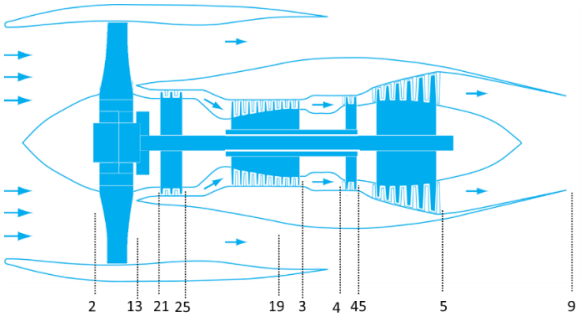

Figure 4: Layout of a very high bypass ratio turbofan engine with station numbers.

Table 1: Performance requirement at various operating conditions.

	Altitude [km]	*Mach number [-]*	*Ambient condition*	*Thrust [kN]*
Cruise	11	0.85	ISA	47
SLS	0	0	ISA+15 K	300
Top of Climb	11	0.85	ISA+15 K	60

The engine performance is modeled using the Gas Turbine Simulation Program (GSP) [18], a modular 0-D thermodynamic modeling environment. The model's layout for an intercooler and ITB turbofan engine is given in Fig. 5. Apart from the main gas path components highlighted by bold numbers, some auxiliary components are used. For instance, the bleed controls (components 2-4, 6-8) specify the cooling mass flow as a fraction of the total air mass flow rate at the inlet of HPC. Component 5 is a thrust scheduler. Table 2 shows the turbomachinery efficiencies and component losses.

An optimizer using a gradient-based method minimizes the cruise thrust specific fuel consumption (TSFC) within the predefined design space while satisfying the thrust requirements and operational limits at hot-day take-off and top of the climb. The operating limits are compressor surge margin and shaft speed.

Table 2: Component efficiencies and pressure losses.

Parameters	*Notations*	*Values*
Fan polytropic efficiency	η_{fan}	0.93
LPC polytropic efficiency	η_{LPC}	0.93
HPC polytropic efficiency	η_{HPC}	0.91
Combustion efficiency	η_{Comb}	0.997
Combustion pressure loss	$\Delta p_{Comb}/p_{t,3}$	0.05
HPT polytropic efficiency	η_{HPT}	0.93
ITB efficiency	η_{ITB}	0.995
ITB pressure loss	Δp_{ITB}	0.03
LPT polytropic efficiency	η_{LPT}	0.925
Duct pressure loss	$\Delta p_{duct}/p_{t,i}$	0.02
Shaft mechanical efficiency	η_{shaft}	0.995

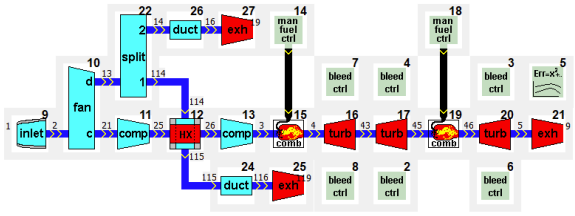

Figure 5: The layout of the engine performance model in GSP.

For the ITB, a constant pressure loss of 3% is considered, and an energy fraction defined in Eqn. (1) is used [10] to adjust the amount of energy input in the ITB concerning the total energy consumption of the engine. Please note the current analysis only uses ITB during the take-off and top of climb phase to minimize the fuel penalty during the cruise.

$$ITB\ energy\ fraction = \frac{\dot{m}_{f_2} \cdot LHV_{f_2}}{\dot{m}_{f_1} \cdot LHV_{f_1} + \dot{m}_{f_2} \cdot LHV_{f_2}} \quad (1)$$

The energy going into the combustion chamber is the product of the fuel lower heating value (LHV) and the fuel flow rate $\dot{m}_f$. The subscript 1 represents the first combustion chamber, and subscript 2 stands for the ITB. The two combustors burn kerosene.

The intercooler is modeled based on a cross-flow configuration between the core and the bypass. The intercooler is used during all flight phases. A split ratio is used to define the amount of bypass flow that goes through the intercooler. The intercooler performance is quantified by its effectiveness, the ratio of actual heat transferred to the maximum allowable heat transfer, as seen in Eqn.(2).

$$e = \frac{\dot{m}_c C_{p,c}(T_{c1} - T_{c2})}{min\{\dot{m}_c C_{p,c}(T_{h1} - T_{c1}), \dot{m}_h C_{p,h}(T_{h1} - T_{c1})\}} \quad (2)$$

where e is the heat exchanger effectiveness; $\dot{m}_c$ and $\dot{m}_h$ are the mass flow rate of the cold and hot flow, respectively; $C_{p,c}$ and $C_{p,h}$ represent the specific heat of the cold and hot flow, respectively; T_c and T_h are the temperature of the cold and hot

flow, respectively; and the subscript 1 and 2 represents the heat exchanger inlet and exit.

The achievable intercooler effectiveness strongly depends on the specific design of the heat exchanger. Since the heat exchanger design is out of this research scope, we employ empirical correlations to calculate the heat transfer rate in the intercooler. Therefore, the temperature difference and the heat exchanger effectiveness. Following this thought, the first step is to calculate the heat transfer coefficient subject to the Nusselt number and the thermal conductivity of the material. The well-known Dittus-Boelter equation [19, 20] in Eqn.(3) is used for the local Nusselt number for turbulent flows inside smooth-surface tubes.

$$N_u = 0.023 \cdot \mathrm{Re}^{0.8} \cdot \mathrm{Pr}^n \tag{3}$$

Where N_u is Nusselt number; R_e is Reynolds number; Pr is Prandtl number; n is 0.4 for heating of the fluid and 0.3 for cooling the fluid. We use the method proposed by Zukauskas [21] to calculate the flow velocity for staggered tube banks and, therefore, the Reynolds number.

Eventually, the cruise effectiveness of 0.5 with the 3% pressure losses on the cold and hot flows is obtained. For the non-cruise conditions, the Reynolds analogy is used to adapt the pressure losses with constant effectiveness of 0.5. According to the Reynolds analogy theory, the pressure loss has a linear dependency on the amount of heat transferred. Therefore, the pressure losses at the take-off condition increase. Such a tendency closely resembles the pressure losses estimated by other studies [18, 21].

2.2 The turbine cooling model

The turbine cooling fraction is estimated based on the empirical model proposed by Jonsson et al. [22], as seen in Eqn. (4).

$$\frac{m_c}{m_g} = b \cdot \frac{C_{p,g}}{C_{p,c}} \cdot \left(\frac{T_g - T_b}{T_b - T_c}\right)^s \tag{4}$$

where m_c is the cooling air mass flow rate in kg/s; m_g is the total mass flow rate of the hot gas in kg/s; $C_{p,g}$ and $C_{p,c}$ are specific heat of gas and cooling air, respectively; T_g is the gas temperature in K; T_b is the maximum allowable metal temperature for turbine stages in K; T_c is the coolant temperature in K; b and s are coefficients related to the effectiveness of the convective cooling and film cooling and to be determined concerning a specific application.

The values of b and s in this analysis are determined using least-squares methods concerning the physics-based cooling model developed by Yin et al. [23]. Eventually, it was found that b equals 1 for stators and equals 0.66 for rotors, whereas the s value will be 1.5 through the whole turbine stages. Figure 6 compares the cooling fraction calculated from the physics-based model in [23] (represented by "literature stator 1" and "literature rotor 1") and the empirical model in Eqn. (1) (represented by "model stator 1" and "model rotor 1"). The values for the HPT rotor and stator are presented separately. The comparison confirms that with the predicted b and s value, the empirical model can capture the turbine cooling characteristics and, therefore, the amount of cooling required.

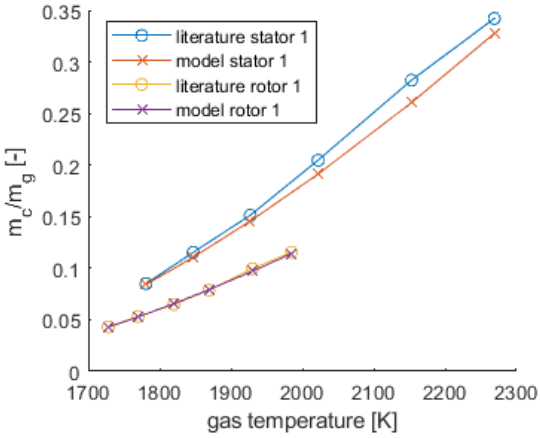

Figure 6: Variation of the cooling fraction for the HPT stages at given turbine inlet temperature (gas temperature). Literature stands for calculation from the physical-based model in [23]; whereas the model stands for the empirical model in Eqn. (1). b = 1 for stators and b=0.66 for rotors; s = 1.5. m_c is cooling mass flow rate and m_g is the total gas mass flow rate at the inlet of the compressor.

In addition, using turbine cooling deteriorates the turbine stage efficiency. This is accounted for by a loss factor, described by Horlock et al.[24] and Wilcock et al.[25]. The cooling loss factor is 0.5, meaning every 1% turbine cooling decreases the polytropic turbine efficiency by 0.5%. This value aligns better with previous literature [26].

2.3 The emission model

CO_2 emissions are calculated based on a complete combustion process and are proportional to the fuel burn. This analysis applies a constant CO_2 emission index of 3.16 kg/kg(fuel) [27].

The NO_x calculation is not straightforward. Depending on the level of fidelity, one can use different approaches. At the conceptual engine phase, empirical methods, e.g., the well-known P_3-T_3 method [7], are good approximations. However, for unconventional engine configurations like the ITB engine, the P_3-T_3 method will not be suitable. Yin and Rao [10] developed a physics-based multi-reactor network to estimate the NO_x emissions of the ITB engine. This method was developed explicitly for RQL combustion and required detailed chemical kinetics for any adaptions, limiting its usage during the engine conceptual analysis.

This research attempts to use a semi-empirical method based on a NO_x severity index (SNO_x) proposed by NASA [28]. The SNO_x is obtained from Eqn. (5).

$$SNO_x = 1.043 \cdot \exp(T_{t3}/194) \cdot FAR^{1.69} \cdot P_{t3}^{0.595} [gNO_x/kgfuel] \tag{5}$$

SNO_x is the NO_x severity index in $g(NO_x)/kg(fuel)$; T_{t3} is the combustor inlet temperature; FAR is the Fuel to Air Ratio; P_{t3} is the total pressure at the combustor inlet. The NO_x emission index ($EINO_x$) is then interpolated based on empirical relations developed by NASA, which is visualized in Fig. 7. For a calculated SNO_x value, the $EINO_x$ can be linearly interpolated

for different combustion techniques, e.g., conventional combustor or dual annular at both cruise and take-off.

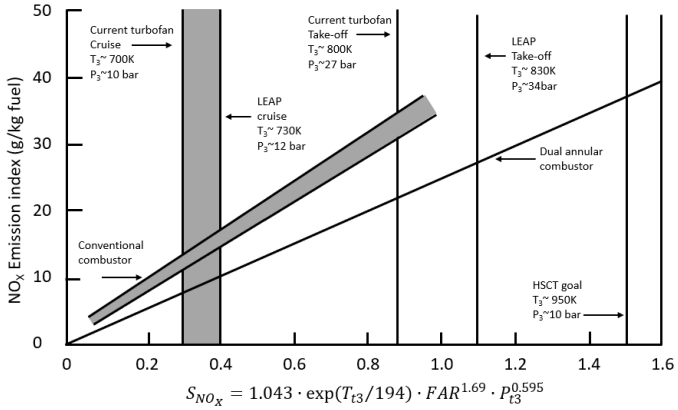

Figure 7: NO_x emission index versus the severity index for NO_x emissions. Figure adapted from [28]

Furthermore, Sullivan's correlation is used to calculate the NO_x emissions from ITB [29]. This correlation approximates the NO_x emissions for reheated engine cycles based on the fuel flow split, the combustion chamber exit temperatures, and the Fuel to Air Ratio at both stoichiometric (*FARs*) and actual conditions. Eqn. (4) shows the calculation details.

$$\frac{NO_x}{NO_{x0}} = y^b(1-y)^b exp\left(\frac{\Delta TIT}{c} - 8.1\alpha\right) \quad (4)$$

where NO_x is the emission value from the reheat system. NO_{x0} is the emission value if fuel were only added into the first combustion chamber, estimated using the SNO_x interpolation method described above. y is the fuel split ratio defined in Eqn. (5) and α is the vitiated air mass ratio defined in Eqn. (6).

$$y = \frac{FAR_1}{FAR_1 + FAR_2} \quad (5)$$

where the subscripts 1 and 2 signify the first and the second combustion chambers, respectively.

$$\alpha = \frac{FAR(1+FAR_S)}{FAR_S - FAR} \quad (6)$$

Where *FAR = FAR1+FAR2*; *FARs = 1/14.7.*

3. RESULTS AND DISCUSSION

3.1 Parametric analysis

We first investigate the sensitivity of engine efficiency and $EINO_x$ to the intercooler effectiveness, pressure losses through intercooler on both cold and hot sides, split ratio of the bypass flow, and the energy split in case of an ITB configuration. The analysis is conducted at cruise conditions with a design space defined in table 3. The engine BPR, FPR, OPR, and HPT inlet temperature optimized by Yin and Rao [10] are taken as the baseline. Also, for the baseline, the heat exchanger effectiveness is 0.5; 10% of the bypass flow is used for intercooling (bypass flow split ratio); the ITB energy fraction is 0.2.

Table 3: Baseline and the variation range of each design parameter.

Parameter	Baseline	Range
Bypass ratio [-]	15	N.A.
Fan pressure ratio [-]	1.44	N.A.
LPC pressure ratio [-]	5	N.A.
HPC pressure ratio [-]	9.7	N.A.
HPT inlet temperature [K]	1900	N.A.
Heat exchanger effectiveness (e) [-]	0.5	0-1
Intercooler pressure loss cold flow [-]	0.05	0-0.2
Intercooler pressure loss hot flow [-]	0.05	0-0.2
Bypass flow split ratio [-]	0.1	0-1
ITB energy fraction [-]	0.2	0-0.5

Figure 8 shows the variation of a): specific thrust, b) Thrust Specific Fuel Consumption, and c) $EINO_x$ versus the heat exchanger effectiveness. The solid line corresponds to the intercooler engine, and the dashed line corresponds to the engine with intercooler and ITB with 80% (first combustor) /20% (ITB) energy split ratio. Increasing the intercooler effectiveness increases the specific thrust, as higher effectiveness means the higher heat transfer rate, hence a colder compression temperature. The OPR and HPT inlet temperature remains constant. Therefore, the available thrust power, thus the specific thrust increases. Also, the engine TSFC increases, but the $EINO_x$ reduces by about 70%. When adding an ITB to the intercooler engine, the overall trend remains the same. In general, the ITB deteriorates the engine performance. It is noticeable that the $EINO_x$ of an intercooler ITB engine is higher than an intercooler engine alone. The reason is that when adding an ITB, the HPT inlet temperature was kept constant intentionally; hence adding an ITB would only produce extra NO_x emissions.

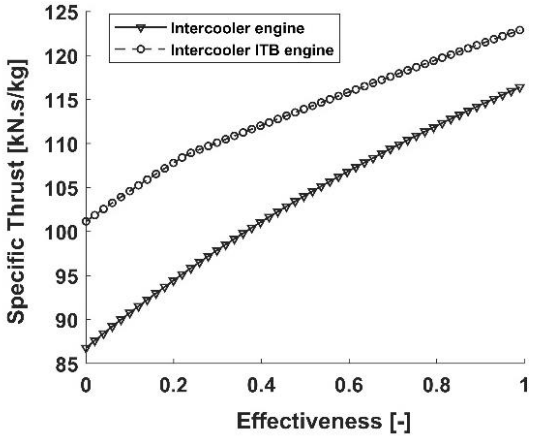

a)

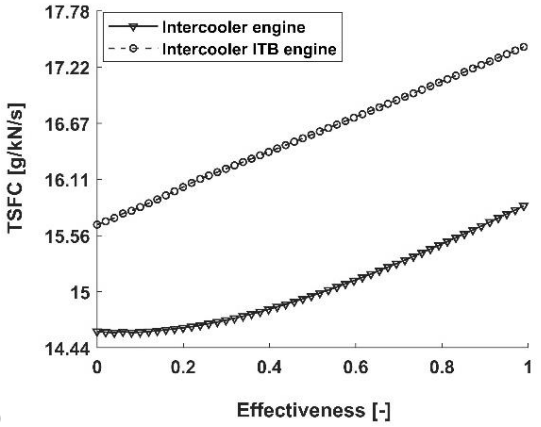

b)

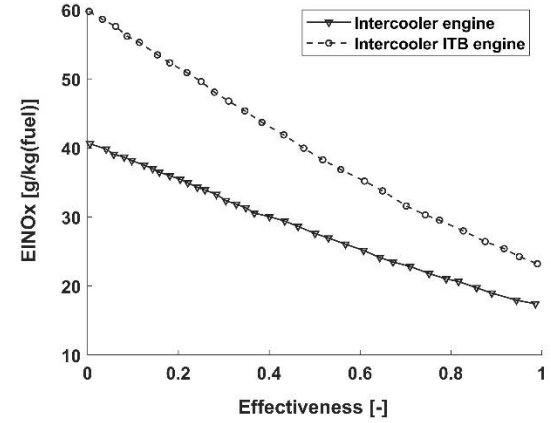

c)

Figure 8: Effect of changing the effectiveness on: a) specific thrust in kN.s/kg; b) TSFC in g/kN/s; c) $EINO_x$ in g/kg(fuel).

Figure 9 and Figure 10 show the variation of specific thrust and TSFC versus the pressure loss on the cold and hot sides of the intercooler, respectively. No effects on $EINO_x$ are expected; therefore, they are not shown. When the pressure loss increases up to 15% of the heat exchanger inlet pressure on both sides, the engine thrust and fuel efficiency decrease. It is noticeable that the pressure loss on the cold side has a more significant effect on the cycle performance than on the hot side.

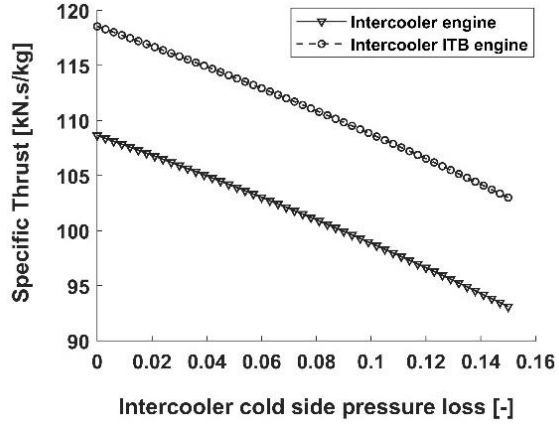

a)

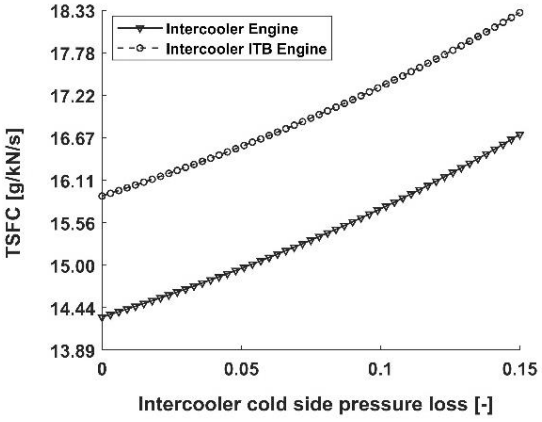

b)

Figure 9: Effect of intercooler cold side pressure loss on: a) specific thrust in kN.s/kg ; b) TSFC (Thrust specific fuel consumption) in g/kN/s.

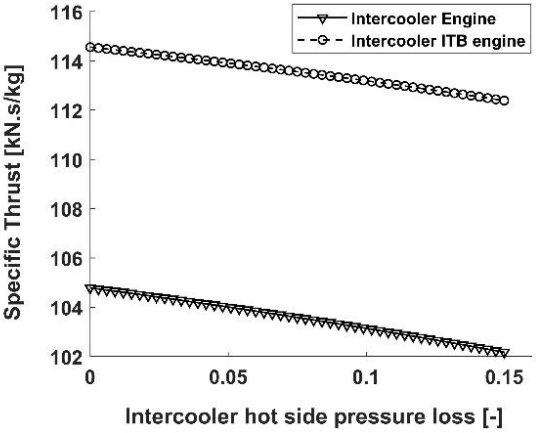

a)

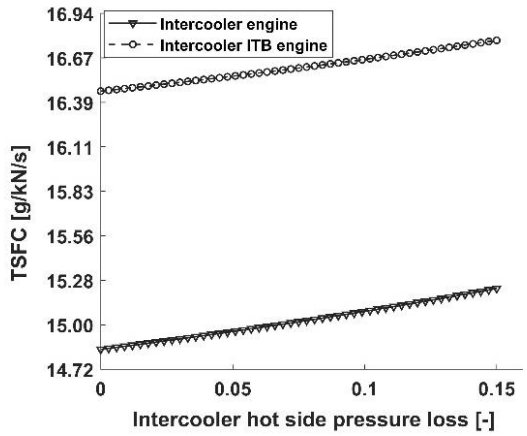

b)

Figure 10: Effect of intercooler hot side pressure loss on: a) Specific Thrust in kN.s/kg; b) TSFC (Thrust Specific Fuel Consumption) in g/kN/s.

Figure 11 shows that increasing the bypass flow split ratio (how much bypass air goes into the intercooler) reduces the thrust and increases the TSFC. Such a trend is expected since more bypass flow is now subjected to the pressure losses while the heat going

into the cold flow stays the same for given effectiveness. No effects on $EINO_x$ are expected.

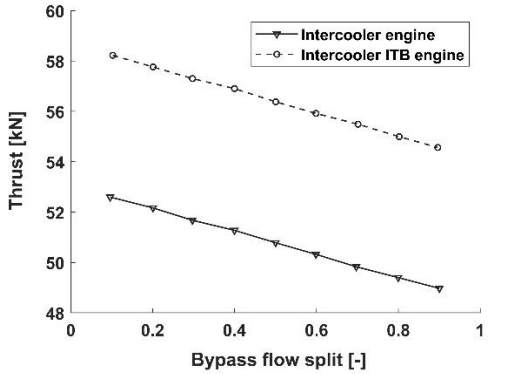

a)

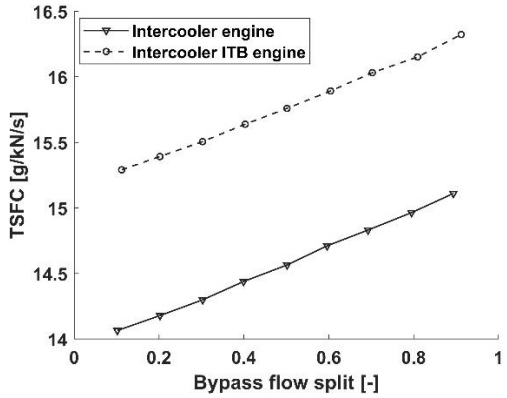

b)

Figure 11: Effect of the bypass flow split ratio on: a) thrust in kN; b) TSFC in g/kN/s.

Increasing the ITB energy fraction increases the specific thrust, as expected (see Fig. 12). This increase diminishes as the ITB energy increases further when the LPT requires cooling. The TSFC increases since fuel is burned at low pressure. The $EINO_x$ also increases, showing contradicting behavior compared to the earlier study [10]. This is mainly because the current parametric analysis has kept the HPT inlet temperature constant. Therefore, increasing the fuel split ratio leads to more fuel in ITB and an increase of LPT inlet temperature, consequently increasing the ITB and the total NO_x emissions. For a constant thrust, one would expect a reduction in HPT inlet temperature, reducing NO_x emissions. This will be verified by the cycle optimization later.

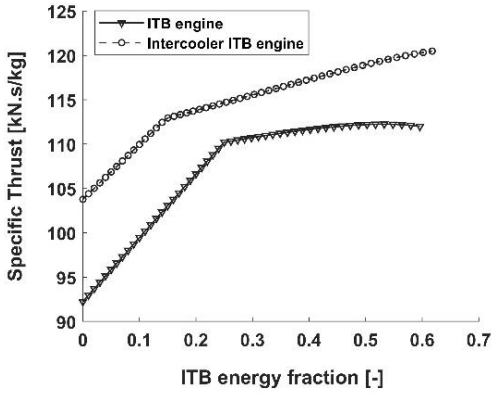

a)

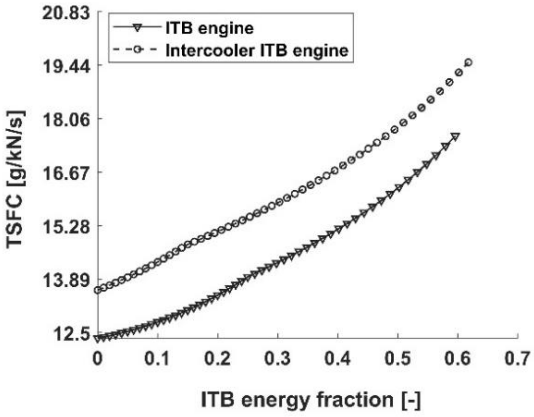

b)

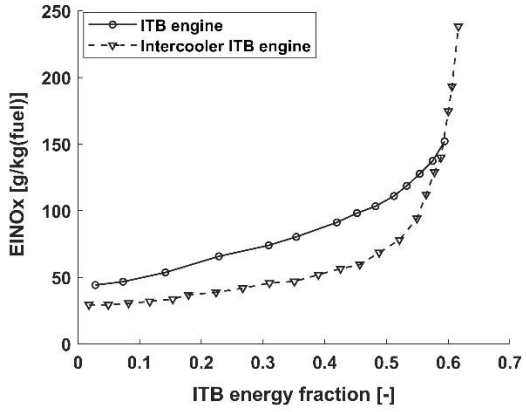

c)

Figure 12: Effect of changing the amount of energy into the ITB (ITB energy fraction) on: a) Specific thrust in kN.s/kg; b) TSFC in g/kN/s; c) $EINO_x$ in g/kg(fuel).

Overall the parametric analysis confirms that intercooling is beneficial to increase the engine specific thrust and decrease the NO_x emissions. The effects of ITB are sensitive to how a cycle is optimized. Using an ITB without reducing the first combustor's fuel consumption would increase the specific thrust, TSFC, and NO_x emissions. Therefore, a careful optimization process is required to reduce NO_x emission from intercoolers and ITB, which will be elaborated on in the next section.

3.2 Performance optimization

The engine performance optimization minimizes the engine cruise TSFC when meeting all the requirements and constraints. The design space can be seen in table 4 and is used for all the engine configurations. For the intercooler engine, the pressure losses of the cold and hot sides are kept constant. For the ITB engine, the ITB is not operated during cruise conditions. At non-cruise conditions, the LPT inlet temperature of the ITB engine is determined by the HPT inlet temperature and the ITB energy fraction. The optimization constraints are the maximum spool speed of 106% and LPT inlet temperature. The specific thrust is kept constant for all engine cycles.

Table 4: Engine optimization space.

Parameter	Baseline	Range
Bypass ratio [-]	15	5-25
Fan pressure ratio [-]	1.44	1-1.8
LPC pressure ratio [-]	5	2-15
HPC pressure ratio [-]	9.7	5-30
HPT inlet temperature [K]	1900	1400-2200
Heat exchanger effectiveness (e) [-]	0.5	0-0.9
Intercooler pressure loss cold flow [-]	0.05	N.A.
Intercooler pressure loss hot flow [-]	0.05	N.A.
Bypass flow split ratio [-]	0.1	0-1
ITB energy fraction [-]	0.2	0-0.4

The intercooler engine is optimized for varying effectiveness from 0.1-0.9 to evaluate the impact a more intrusive intercooler has on the cycle. Figure 13 shows the variation of the engine (a) TSFC and (b) $EINO_x$ of cruise and take-off concerning the intercooler effectiveness. Overall, the TSFC and $EINO_x$ decrease as the heat exchanger effectiveness increases due to the reduced HPT exit temperature. However, the block fuel burn might show a different trend as increasing the heat exchanger effectiveness will increase weight. Kyprianidis et al. [30] show that increasing the intercooler effectiveness at take-off from 0.7 to 0.8 causes an increase of intercooler weight by up to 40%, which might increase the block fuel by up to 0.7%. Further analysis should be performed to analyze the weight impact.

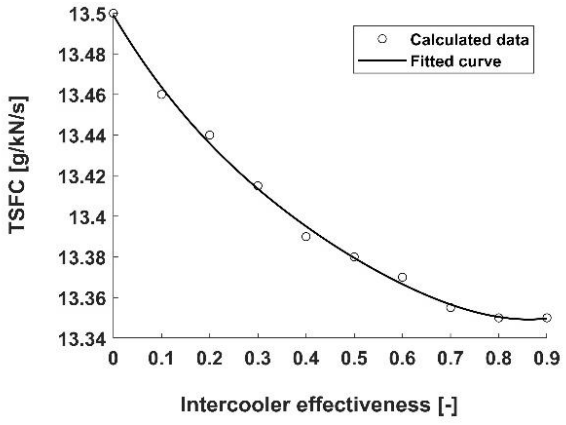

a)

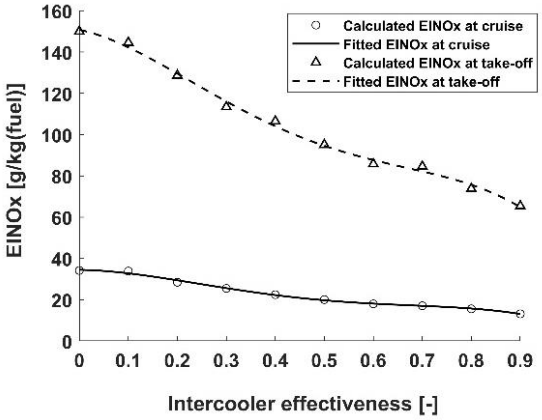

b)

Figure 13: Sensitivity of the a) TSFC in g/kN/s and b) $EINO_x$ in g/kg(fuel) to the intercooler effectiveness.

The ITB engine cycle is optimized with varying ITB energy fractions from 0-0.4 at take-off. Figure 14 shows the variation of a) cruise TSFC, (b) cruise $EINO_x$, and (c) take-off $EINO_x$ versus the ITB energy fraction at take-off. It is noticeable that operating the ITB with a 0.2 energy fraction allows the minimum TSFC to be achieved; however, further increasing the ITB energy fraction reduces the $EINO_x$. A proper tradeoff between fuel efficiency and NO_x emissions is therefore essential.

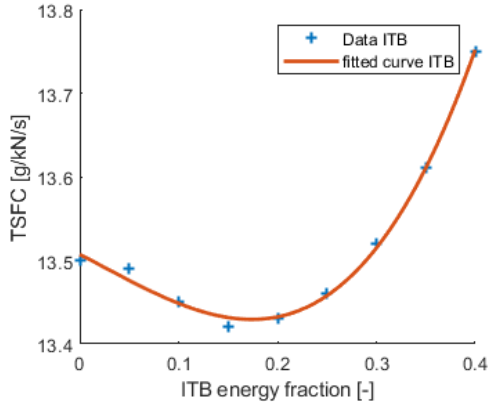

a)

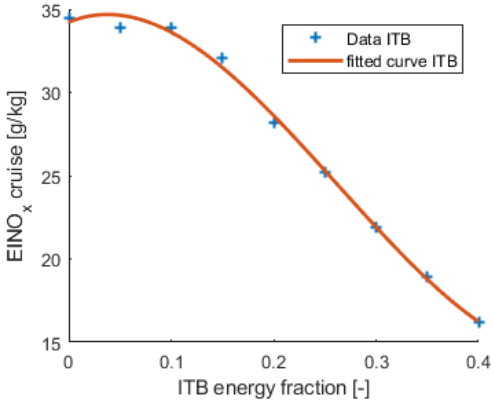

b)

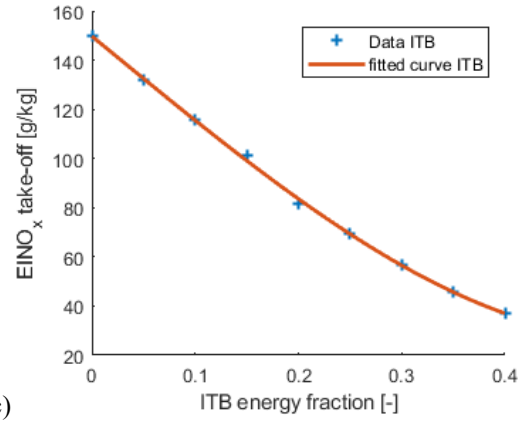

c)

Figure 14: The variation of a) engine cruise TSFC in g/kN/s; b) cruise EINO$_x$ in g/kg(fuel); and c) take-off EINO$_x$ in g/kg(fuel) versus ITB energy fraction.

For the intercooler ITB engine, the combined effects on engine performance and NO$_x$ emissions are studied. Figure 15 shows the variation of a) cruise TSFC, (b) cruise EINO$_x$, and (c) take-off EINO$_x$ versus the changes of take-off ITB energy fraction and the heat exchanger effectiveness. A local minimum TSFC occurs at the effectiveness of 0.3 and the ITB energy fraction of 0.15; however, the global minimum cruise TSFC is obtained at the maximum heat exchanger effectiveness. Furthermore, the cruise EINO$_x$ is dominated by the heat exchanger effectiveness, as the ITB is not in use. At take-off, the minimum EINO$_x$ occurs at the heat exchanger effectiveness of 0.7, with the ITB energy fraction varying between 0.1 to 0.25.

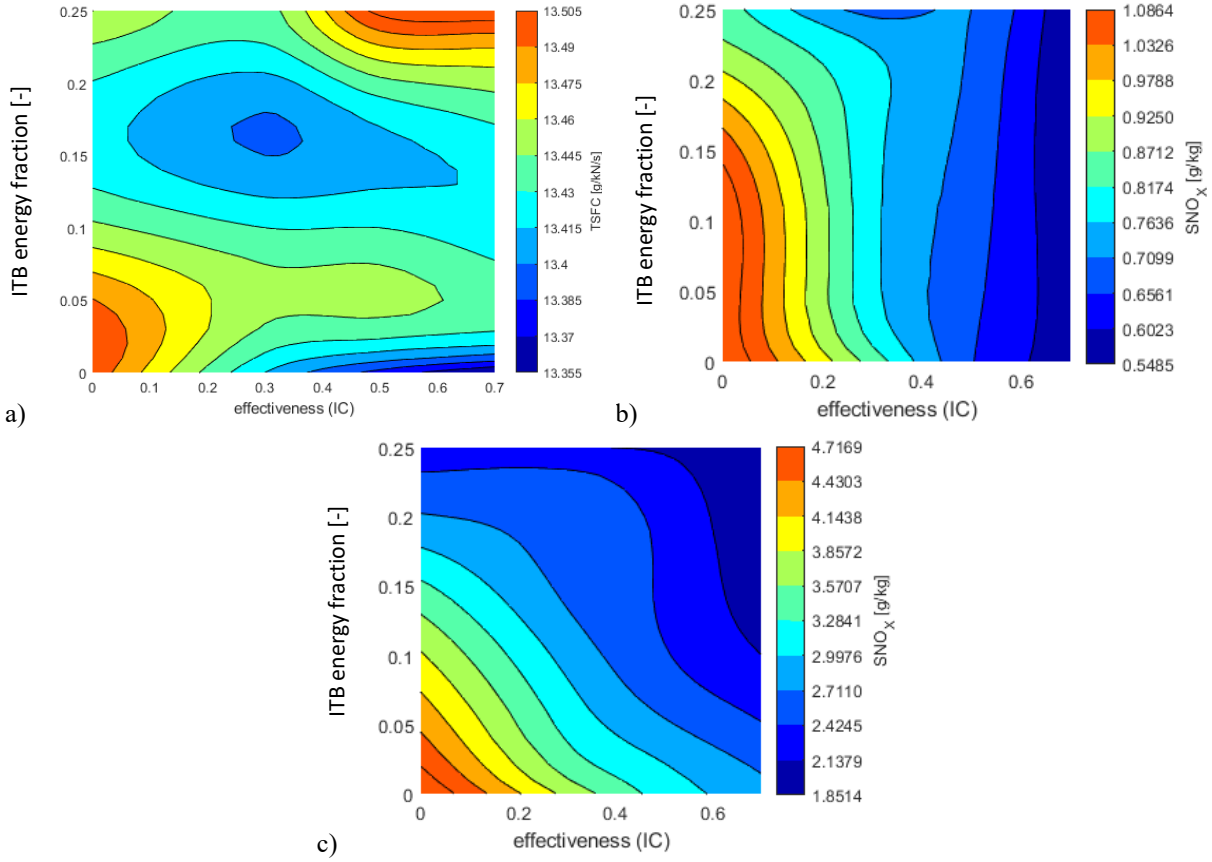

a) b) c)

Figure 15: Changes of a) cruise TSFC; b) cruise SNO$_x$; and c) take-off SNO$_x$ versus the take-off ITB energy fraction and the intercooler effectiveness for the intercooler ITB engine.

From the full range of optimization, we conclude that ITB should be operated with the energy split of 85%(first burner)/15%(ITB) at take-off to minimize the cruise TSFC and cruise NO$_x$ emission is more sensitive to the heat exchanger effectiveness. As for the intercooler engine, in principle, increasing the intercooler effectiveness always reduces the engine's TSFC and NO$_x$ emissions. For the intercooler ITB engine, the intercooler effectiveness of 0.3 combined with an ITB energy fraction of about 0.15 can well balance the TSFC and NO$_x$ emissions.

Table 5 shows an example of the selected engine cycles for different engine architectures at cruise. If an intercooler is in use, the heat exchanger effectiveness is 0.5. As for the ITB in use, the ITB energy fraction is 0.25 at take-off and 0 at cruise. Overall, the four engines have similar OPR; however, the intercooler engine favors the higher HPC pressure ratio split. The BPR of

the intercooler engine increases by about 30% than the baseline engine. The cruise TSFC is slightly reduced by 0.5% to 0.8% compared to the baseline engine. Nevertheless, we expect the $EINO_x$ to be 16% lower for the intercooler engine, 26% lower for the ITB engine, and 38% lower for the intercooler-ITB engine than the baseline engine.

Table 5 Optimized engine performance at cruise: altitude = 11km; Mach number = 0.85; thrust = 47kN; heat exchanger effectiveness = 0.5; the ITB is not in use.

Parameter	Baseline engine	Intercooler engine	ITB engine	Intercooler ITB engine
Total air mass flow rate [kg/s]	498.1	499	499	499
BPR [-]	12.13	15.4	12.07	13.88
OPR [-]	63.89	63.68	63.82	63.73
FPR [-]	1.46	1.45	1.45	1.45
LPC PR [-]	4.83	2.79	4.38	2.34
HPC PR [-]	9.08	16.27	10.06	19.41
HPT inlet temperature [K]	1568	1625	1466	1480
LPT inlet temperature [K]	NA	NA	1070	1050
HPT cooling fraction [%]	19.08	18.09	4.47	5.85
LPT cooling fraction [%]	0	0	0.31	0.18
TSFC [g/kN/s]	13.84	13.73	13.77	13.75
$EINO_x$ cruise [g/kg(fuel)]	26.4	22.2	19.5	16.5

Figure 16 summarizes the variation of engine TSFC and $EINO_x$ to the baseline engine at take-off. At take-off, using the ITB provides operational flexibility. In Fig. 16, the blue bar shows the situation where ITB is not used (ITB energy fraction=0), whereas the orange bar shows the ITB energy fraction of 0.25. Increasing the ITB energy fraction reduces cycle efficiency by up to 11% but enables the substantial reduction of NO_x by nearly 55%.

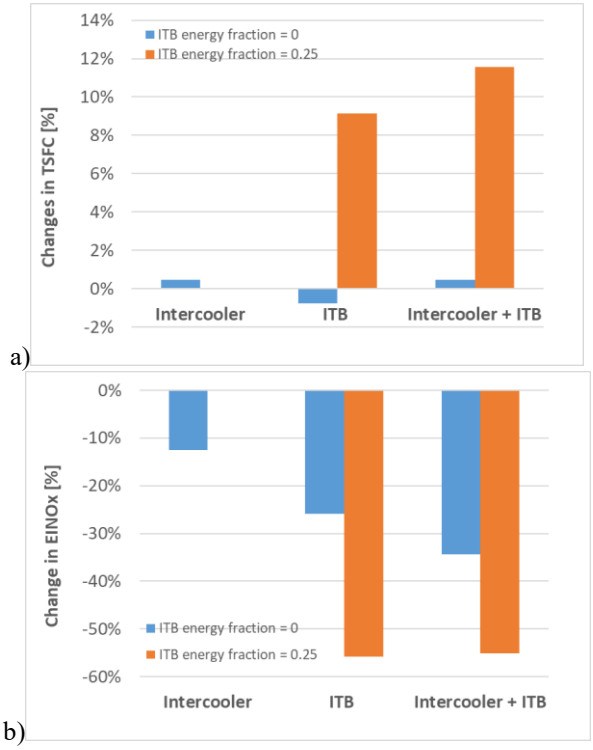

Figure 16: Changes of the engine a) TSFC and b) $EINO_x$ to the baseline turbofan engine during take-off.

4. CONCLUSION

This paper studies the potential of an intercooler and ITB engines on reducing NO_x emissions without having adverse effects on fuel efficiency. From the analysis, the following conclusions can be drawn.

- Both intercooler and ITB can reduce NO_x emissions. Separately, the NO_x emission is reduced by 16% for the Intercooler and 26% for ITB. Combining the two components allows the reduction to 38% compared to a baseline VHBR engine.
- During take-off, the ITB offers an extra degree of freedom that allows for an even higher reduction of NO_x emissions (up to 55%) at the cost of increased fuel consumption.
- Using intercooler and ITB can effectively decouple the dependency of thermal NO_x on the engine pressure ratio, hence allowing the reduction of NO_x without penalizing the fuel efficiency.
- The installation effects of ITB should be looked into as the size and weight of the ITB turbofan with intercooler is more than a conventional two-spool turbofan engine.

ACKNOWLEDGEMENTS

The individual author of this work receives funding from the Dutch Research Council (NWO) under the talent scheme VENI. The project number is 17367.

REFERENCES

1. Airbus, *Global Market Forecast: Global Networks, Global Citizens 2018-2037*. 2018, Airbus: Toulouse, France.
2. Lee, D.S., D.W. Fahey, A. Skowron, M.R. Allen, U. Burkhardt, Q. Chen, S.J. Doherty, S. Freeman, P.M.

Forster, J. Fuglestvedt, A. Gettelman, R.R. De León, L.L. Lim, M.T. Lund, R.J. Millar, B. Owen, J.E. Penner, G. Pitari, M.J. Prather, R. Sausen, and L.J. Wilcox, *The contribution of global aviation to anthropogenic climate forcing for 2000 to 2018.* Atmospheric Environment, 2021: p. 117834.
3. ACARE, *Flightpath 2050 Europe's vision for aviation*. 2011: European Commission.
4. Yin, F. and A.G. Rao, *A Review of Gas Turbine Engine with Inter-stage Turbine Burner.* Progress in Aerospace Sciences, 2020. **121**.
5. ICAO, *Report of the Independent Experts on the LTTG NOx Review and Medium and Long Term Technology Goals for NOx*. 2008: Montréal: International Civil Aviation Organization.
6. Perpignan, A.A.V., A. Gangoli Rao, and D.J.E.M. Roekaerts, *Flameless combustion and its potential towards gas turbines.* Progress in Energy and Combustion Science, 2018. **69**: p. 28-62.
7. Norman, P.D., D.H. Lister, M. Lecht, P. Madden, K. Park, O. Penanhoat, C. Plaisance, and K. Renger, *Development of the Technical Basis for a New Emissions Parameter Covering the Whole Aircraft Operation: NEPAIR*. 2003.
8. Kyprianidis, K.G., T. Grönstedt, S.O.T. Ogaji, P. Pilidis, and R. Singh, *Assessment of Future Aero-engine Designs With Intercooled and Intercooled Recuperated Cores.* Journal of Engineering for Gas Turbines and Power, 2011. **133**(1): p. 011701.
9. Gronstedt, T. and K. Kyprianidis. *Optimizing the Operation of the Intercooled Turbofan Engine*. in *ASME Turbo Expo 2010: Power for Land, Sea, and Air*. 2010.
10. Yin, F. and A.G. Rao, *Performance analysis of an aero engine with inter-stage turbine burner.* The Aeronautical Journal, 2017. **121**(1245): p. 1605-1626.
11. Sirignano, W.A. and F. Liu, *Performance Increases for Gas-Turbine Engines Through Combustion Inside the Turbine.* Journal of Propulsion and Power, 1999. **15**(1): p. 111-118.
12. Liu, F. and W.A. Sirignano, *Turbojet and turbofan engine performance increases through turbine burners.* Journal of Propulsion and Power, 2001. **17**(3): p. 695-705.
13. Liew, K.H., E. Urip, S.L. Yang, J.D. Mattingly, and C.J. Marek, *Performance Cycle Analysis of Turbofan Engine with Interstage Turbine Burner.* Journal of Propulsion and Power, 2006. **22**(2): p. 411-416.
14. Perpignan, A.A.V. and A. Gangoli Rao, *Effects of chemical reaction mechanism and NOx formation pathways on an inter-turbine burner.* The Aeronautical Journal, 2019. **123**(1270): p. 1898-1918.
15. Rao, A.G., F. Yin, and J.P. van Buijtenen, *A hybrid engine concept for multi-fuel blended wing body.* Aircraft Engineering and Aerospace Technology, 2014. **86**(6).
16. Yin, F., A. Gangoli Rao, A. Bhat, and M. Chen, *Performance assessment of a multi-fuel hybrid engine for future aircraft.* Aerospace Science and Technology, 2018. **77**: p. 217-227.
17. Perpignan, A.A.V., M.G. Talboom, Y. Levy, and A.G. Rao, *Emission Modeling of an Interturbine Burner Based on Flameless Combustion.* Energy & Fuels, 2018. **32**(1): p. 822-838.
18. Visser, W.P.J. and M.J. Broomhead, *GSP A generic object-oriented gas turbine simulation environment*. 2000.
19. Dittus, F.W. and L.M.K. Boelter, *Heat transfer in automobile radiators of the tubular type.* International Communications in Heat and Mass Transfer, 1985. **12**(1): p. 3-22.
20. Winterton, R.H.S., *Where did the Dittus and Boelter equation come from?* International Journal of Heat and Mass Transfer, 1998. **41**(4): p. 809-810.
21. Žukauskas, A., *Heat Transfer from Tubes in Crossflow.* Advances in Heat Transfer, 1972. **8**: p. 93-160.
22. Jonsson, M., O. Bolland, D. Bucker, and M. Rost, *Gas turbine cooling model for evaluation of novel cycles*, in *ECOS 2005*. 2005: Trondheim, Norway.
23. Yin, F., F.S. Tiemstra, and A.G. Rao, *Development of a Flexible Turbine Cooling Prediction Tool for Preliminary Design of Gas Turbines.* Journal of Engineering for Gas Turbines and Power, 2018. **140**(9).
24. Horlock, J.H., D.T. Watson, and T.V. Jones, *Limitations on Gas Turbine Performance Imposed by Large Turbine Cooling Flows.* Journal of Engineering for Gas Turbines and Power, 2001. **123**: p. 487-494.
25. Wilcock, R.C., J.B. Young, and J.H. Horlock, *The Effect of Turbine Blade Cooling on the Cycle Efficiency of Gas Turbine Power Cycles.* Journal of Engineering for Gas Turbines and Power, 2005. **127**: p. 109-120.
26. Yin, F. and A.G. Rao, *Performance analysis of an aero engine with inter-stage turbine burner.* The Aeronautical Journal, 2017. **121**: p. 1605–1626.
27. Lefebvre, A.H.A.H. and D.R. Ballal, *Gas turbine combustion : alternative fuels and emissions* 2010 Boca Raton, FL : CRC Press
28. Council, N.R., *Aeronautical Technologies for the Twenty-First Century*. 1992, Washington, DC: The National Academies Press.
29. Sullivan, D.A., *A simple gas turbine combustor NO x correlation including the effect of vitiated air.* Journal of Engineering for Power, 1977.
30. Kyprianidis, K.G., *Multi-disiplinary conceptal design of future jet engine systems*, in *Department of Power and Propulsion*. 2010, Granfield University.